Materials Research Proceedings 28 (2023) 277-284 https://doi.org/10.21741/9781644902479-30

XCT-based microscale analysis of structure and deformability of abdominal wall meshes

SOETE Jeroen[1,a *], MAES Arne[1,2,3,b], ROJAS Camilo[1,c], KYOSEV Yordan[4,d], SCHMIDT Ann-Malin[4,e], LOMOV Stepan V.[1,f], MISEREZ Marc[5,g], KERCKHOFS Greet[1,2,3,6,h] and WEVERS Martine[1,i]

[1] Dept of Materials Engineering, KU Leuven, Leuven, Belgium

[2] Biomechanics lab, Institute of Mechanics, Materials and Civil Engineering, UCLouvain, Louvain-la-Neuve, Belgium

[3] Pole of Morphology, Institute of Experimental and Clinical Research, UCLouvain, Brussels, Belgium

[4] Institut für Textilmaschinen und Textile Hochleistungswerkstofftechnik, TU Dresden, Dresden, Germany

[5] Dept. of Abdominal Surgery, University Hospital Gasthuisberg, Leuven, Belgium

[6] Prometheus, Division for Skeletal Tissue Engineering, KU Leuven, Leuven, Belgium

[a]jeroen.soete@kuleuven.be, [b]arne.maes@kuleuven.be, [c]camilo.rojas@kuleuven.be, [d]yordan.kyosev@tu-dresden.de, [e]ann-malin.schmidt@tu-dresden.de, [f]stepan.lomov@kuleuven.be, [g]marc.miserez@kuleuven.be, [h]greet.kerckhofs@uclouvain.be, [i]martine.wevers@kuleuven.be

Keywords: XCT, Knitted Textiles, Synthetic Meshes, Abdominal Wall Hernia Repair

Abstract. Abdominal wall hernia repair mostly involves the implantation of a synthetic mesh material. The link between the mesh microstructure, mechanical behaviour and clinical outcome is still not fully understood, complicating the selection of a suitable patient-specific mesh. Here, we created a parametric 3D model of a synthetic mesh based on X-ray microfocus computed tomography (XCT) images. The model was implemented in a *TexMind* Warp Knitting Editor software and then exported for finite element model (FEM) analysis. This model allows better understanding of the mechanical behaviour of the mesh and identifying the influence of single structural parameters that are essential for the design of the mesh. We also used the XCT-based filament paths to directly build a FEM, representing all 3D structural details of the as-produced product. Whilst the mechanical analysis of the mesh is feasible, important difficulties are identified, related to the initial relaxed mesh contacts configuration and necessity of the mesh pretension in experiments and calculations.

Introduction

An abdominal hernia is a medical condition in which an internal organ partially protrudes through the surrounding structures, i.e. the musculofascial layers of the abdominal wall. There is a lifetime risk for inguinal hernia of about 27% for men and 3% for women. Consequently, abdominal wall hernia repair is among the most frequently performed surgeries, and it is mostly performed on adults younger than 65 years old [1]. Hernia repair involves in most cases the implantation of a synthetic mesh material to substantially reduce the rate of hernia recurrence [2,3]. Nowadays, a wide range of mesh types is available for the surgeon to choose from in terms of polymer type (degradable or not), fibre structure (mono- vs. multifilament), textile structure (woven vs. knitted), strength, stiffness, elasticity, pore size, weight per area, etc. [4]. Depending on the manufacturing process, synthetic meshes can be divided in woven, non-woven or knitted (weft or warp).

Nowadays, however, most commercially available meshes are fabricated by warp-knitting since it allows to achieve the desired mesh properties, both structurally and biomechanically [5].

Clinical outcome and postoperative quality of life are strongly influenced by the structural and biomechanical properties of the mesh, [6]. Biomechanically, the mesh should ideally behave in a similar manner to the native tissues of the abdominal wall, whilst being able to withstand the *in vivo* mechanical loads, as internal abdominal pressure can reach values up to 20 kPa [7]. Current mesh designs generally can withstand the high forces within the abdominal wall, but often have anisotropic characteristics concerning elasticity. In that case, mesh positioning should conform to the elasticity of the abdominal wall. However, many of the biomechanical tests used in vitro for the mechanical characterization of synthetic meshes currently still lead to inconsistent and non-robust results. Only scarce information is available on the biomechanical behaviour of the meshes after implantation, which if present strongly relates to the biocompatibility of the material and consequent tissue ingrowth. There is, hence, a need for better understanding of the structural changes during loading and the in vivo effects on mechanical properties of the meshes to be able to improve their design.

State-of-the Art of Warp-Knitted Meshes Modelling and Mechanical Characterisation

The warp knitting technology provides a unique possibility to produce structures, which satisfy all technical requirements for hernia repair [8, 9]. Especially the mesh type fabrics produced by fine mono-filaments have excellent seam slippage characteristics – the longer chains of loops remains stable during deformation [10]. At the same time knitted meshes provide a reduced contact area with a foreign body, hence decreasing the risk for granuloma bridging and providing sufficient open space for tissue ingrowth [11].

The mechanical response of surgical warp-knitted meshes is studied in [12-15]. The mesh biaxial tension and shear mechanical response is studied experimentally in these papers (including *in-vivo* measurements). In [16] the mechanical response of the mesh represented as a membrane is modelled, which advances this work towards a model of a warp-knitted loops in a mesh structure. These developments are included in a general "landscape" of geometrical and mechanical models of warp-knitted fabrics [17-20]. The available geometrical models create an idealized 3D sketch of the fabrics, which does not represent the relaxed state of the material and has to be refined using mechanical modelling with finite element method (FEM).

X-ray Microfocus Computed Tomography (XCT) provides the opportunity for direct observation and modelling of the 3D geometry of textiles [21], including knitted fabrics [22] in a relaxed or loaded state. In the present paper we compare parametric FEMs of a warp-knitted surgical mesh created using the *TexMind* software [20] and a "digital twin" of the real mesh, with an XCT-based FEM. These fine-tuned parametric models would allow optimization of the surgical mesh in future work.

Developments of the XCT-based geometrical models and simulation of their mechanical behaviour is well-aligned with similar studies of the composite reinforcements under forming [23].

Materials

A DynaMesh®-CICAT Visible mesh (FEG Texiltechnik, Aachen, Germany) was used in this study. This mesh is designed for the extraperitoneal repair of primary ventral (umbilical, epigastric) and incisional hernias [24]. This anisotropic large pore surgical mesh is a monofilament (+/- 100 μm) polyvinylidene fluoride (PVDF, grade SOLEF 1008 of Solvay Solexis) mesh with black orientation strips (Fig. 1a) that act as guides in the correct positioning of the implant during surgery, for conforming to the elasticity of the abdominal wall. Moreover, the black orientation filaments, are impregnated with iron oxide for allowing MRI visibility of the mesh. The PVDF filaments provide good biocompatibility, as they induce less granuloma formation and are less affected by degradation and embrittlement when compared to their polypropylene-based

counterparts [25, 26]. The warp-knitting pattern used in this mesh is the key to tear propagation resistance and provides the desired high porosity of the mesh.

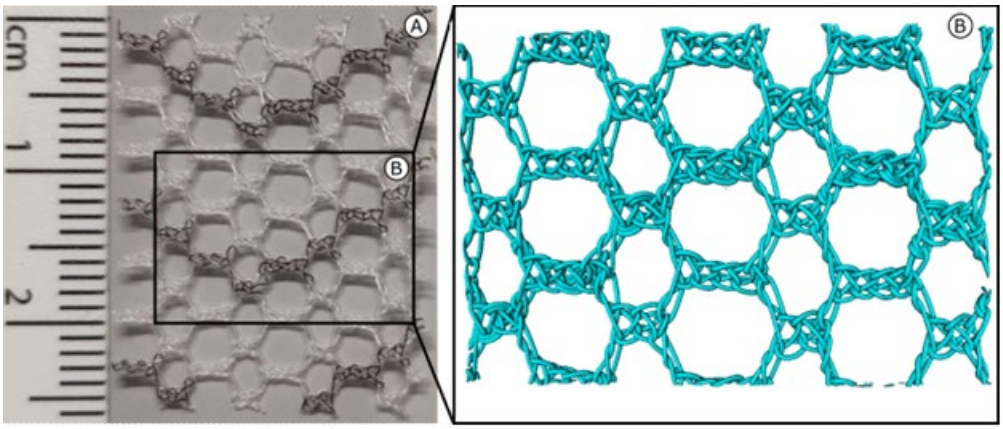

Fig. 1. The surgical mesh DynaMesh®-CICAT: (a) a photo; (b) XCT 3D rendering.

XCT Registration and Analysis of the Mesh 3D Image

A 2 cm by 2.5 cm piece of the DynaMesh®-CICAT surgical mesh was placed in between two half-cylinder Styrofoam parts to keep the fabric straight, while preserving a relaxed state. The assembly was slid into a polysulfone (PSU) sample holder and mounted on the rotation stage of a Bruker SkyScan 1172 scanner, equipped with a closed Hamamatsu 100 kV/10 W microfocus X-ray tube, and a 12-bit detector of 4000 × 2700 pixels. The acquisition parameters are listed below (Table 1). Cross-sectional imaging reconstruction was performed by applying a filter back-projection algorithm in the BRUKER SkyScan software NRecon, with a post-alignment filter to optimize the center of rotation value and a median filter to improve the signal to noise ratio.

Table 1. XCT acquisition parameters.

Tube Voltage [kV]	37	Detector Rows	1332
Tube vCurrent [µA]	234	Detector Columns	2000
Tube Power [W]	8,7	Exposure timing (ms)	215
Hardware filter	None	Voxel size (µm)	8,94
Rotation step [deg]	0,4	Frame Averaging	3
Sector scan [deg]	180	Random movement	ON
Detector binning	2x2		

XCT-based 3D voxelized structures are not suitable as input for mechanical modelling as the voxels create stepped surfaces, which result in an unrealistic and erroneous mechanical behavior in the modelling. Therefore, the aim was to perform a finite element meshing of each individual filament in the surgical mesh structure, extracted using the Avizo XFiber module (Fig. 1b), allowing to obtain smooth filament surfaces.

Transformation of the XCT Dataset Into a FE Model

The transformation of the XCT dataset into a parametric FEM started with the processing of the filament segment nodes and points, by visual inspection of the location and interpenetrations. The original points that represent each filament segment are replaced with interpolated points, with an inter-point distance of 178 µm. This distance allows representing the filament segment without

over-constraining the spline or losing information. The distance is controlled by the smaller radius of curvature, where more points are needed.

With the new equidistant points, a spline is created that serves as the base for a path pultrusion, allowing the creation of each individual yarn. It is possible that for some tight curvature radii, a spline can be created, but a pultrusion of the specified fibre diameter will not provide realistic results, as it generates self-penetrating fibres. Here, having the equidistant points comes in handy, as it is possible to manually edit the points in question and reduce the curvature radius.

To reduce the required computational resources, a general element size of 100 µm was used in the model. One fibre had a high curvature, forcing to reduce the element size to 20 µm, to avoid negative volumes (Fig. 2a, inset). The boundary conditions were set for biaxial tension (Fig. 2b).

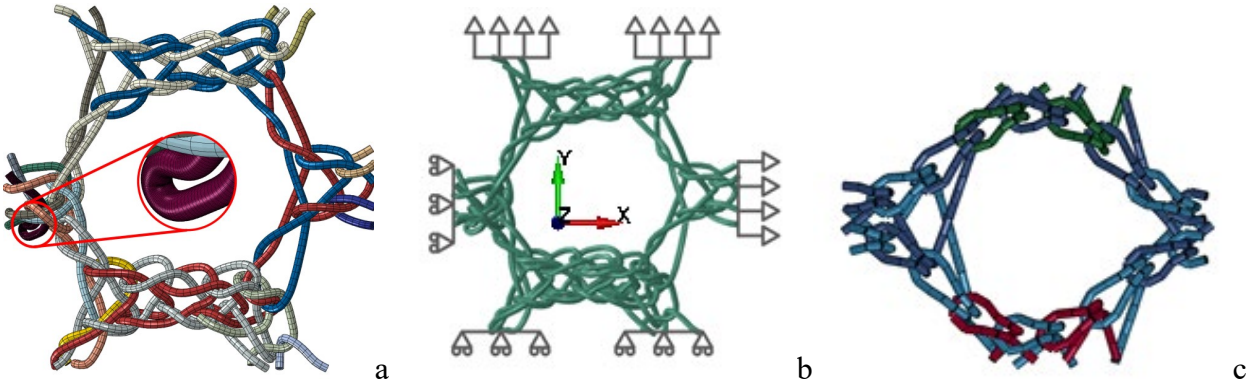

Fig. 2. FE models based on the XCT image, Abaqus (a), with boundary conditions for biaxial tension (b), and exported from TexMind for LS Dyna (c).

Parametrical Modelling of the Warp Knitted Structures

Fig. 3 shows the knitting pattern and the idealised geometrical model of the warp-knitted mesh. Depending on the run-in settings on the machine (derived yarn length per 480 loops) and the bending stiffness of the monofilament yarns the loops will be formed with different geometry. A more stiff filament, at sufficiently large yarn length, forms wider loops, while lower yarn length per loop, and material with lower bending rigidity, forms narrow loops. The yarn length per loop influences the possibility for slippage of the yarn during deformation, and in this way wider and larger loops will result in a larger initial elongation and a lower elasticity modulus.

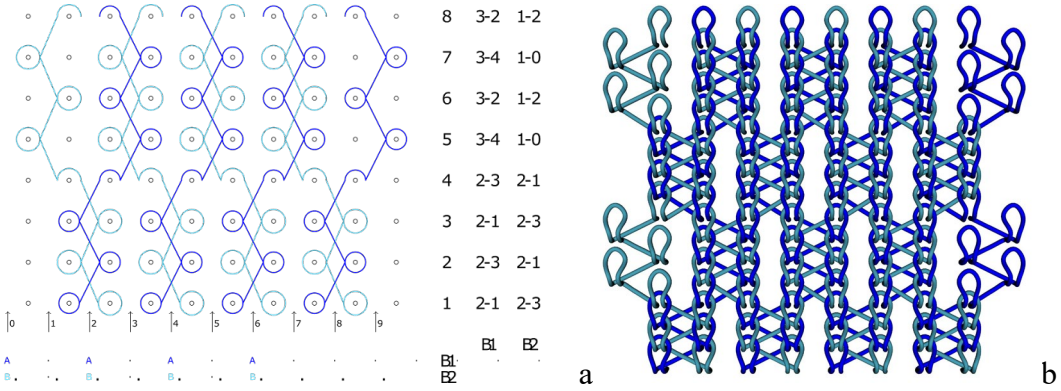

Fig. 3. Pattern of common warp knitted fabrics for production of hernia mesh, lapping and threading notation (a), idealised geometrical model (b), by TexMind Warp Knitting Editor [20].

The idealized geometrical model can be refined by adjusting the loop centre position in the horizontal direction, based on the sum of the horizontal projections of the resulting forces of all

yarns during the knitting process, the flexibility or stiffness coefficient and a scaling factor [19]. Fig. 4 represents the reconstructed FE geometry of one unit cell of the investigated mesh structure, compared with the parametrically modelled one. From the XCT image the yarns can be well-recognized. The loops move not only around the horizontal axis, but they rotate as well under the influence of the yarn tension. Such a rotation of the knitted cells is not implemented yet in the parametrical model, but this can be an extension of the model in the future, in a similar way as the correction of the horizontal loop centre position.

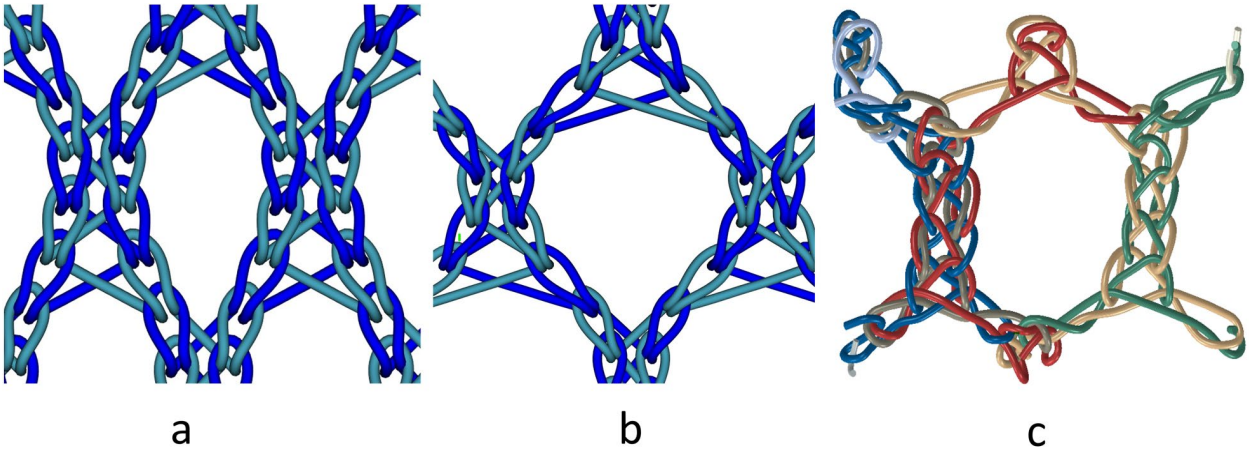

Fig. 4. Comparison of the parametrically modelled structure, two different machine gauges (a,b) with the one obtained by XCT analysis (c).

The parametric modelling of the warp knitted structure is performed without information about the available yarn length per loop. Two figures with different machine gauge (spacing between the needles) and level of side deformation are visualised at Fig. 4a and 4b and they still have different configurations than the reconstructed geometry Fig.4c. The reconstructed geometry shows longer loops in the transition areas between the single linear elements, which can be achieved as well with larger run-in for these steps on computer-controlled machines. For the proper modelling in such case an iterative process with variation of the loop length per each loop and comparison of the simulated and extracted geometry is required, but its implementation is a complex procedure.

The modelled warp knitted fabrics store the coordinates of the single yarns in the memory and as files with lists of 3D coordinates. During the application of explicit FEM software for the modelling process, the element length influences the integration time step. In order to keep all elements with equal length, the curves of the yarn paths are fitted with cubic splines, and then starting from the first node of each yarn, the next node for export for FEM is located from the yarn path so, that the element length remains constant to the value, specified by the user (0.25 mm in this case). The computed nodal coordinates are saved as a text file for LS-Dyna or Abaqus, with the required format as nodes, and then elements between these are placed by interpolation. The complete process is implemented as C++ library, using The Visualization Toolkit (VTK) for visualisation and processing. The model exported in LS Dyna is shown in Fig. 2c.

Modelling of the Biaxial Tension of the Mesh

Biaxial tension on X and Y directions with the equal displacements U_0 on the two axes was applied in LS Dyna to the FE model, exported from *TexMind* and in Abaqus for the XCT-based model. Fig. 5 shows the calculated displacement – force diagrams. The initial regions with low resistance are corresponding to the regime of unbending of the filaments and transition of the loops to the locked condition. In XCT-based model, Fig. 5a, this region exhibits certain resistance to loading, albeit low. For the loading in X direction this low stiffness behavior continues till the end of the

calculation. The inset in Fig. 5b shows details of this region for *TexMind* model. The jumps and negative force values correspond to the resolving of contacts caused by the sliding of the yarns. The forces in this region in this model should be taken as zero. After the loops are locked, the resistance is given by the elongation of the yarns.

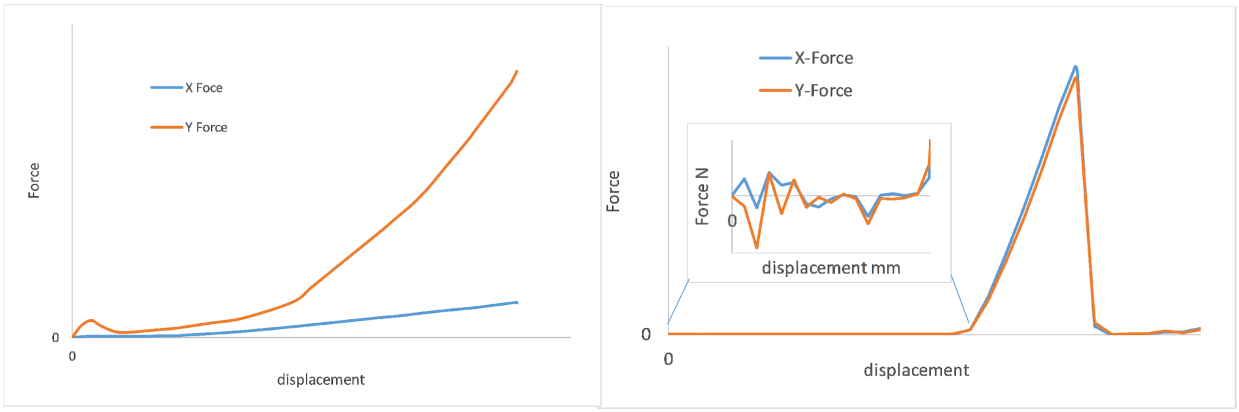

Fig. 5. Biaxial tension diagrams, calculated for the XCT-based digital twin in Abaqus (a) and for the idealised model in LS Dyna (b).

The graphs in Fig. 5 are plotted without specification of the absolute values of force and displacement, because in the present calculations FE convergence problems have forced us to use quite arbitrary values for the filaments and contact properties, based on the FE convergence requirements rather than on the physics. However, the present results allow making certain observations, which highlight difficulties in achieving true-to-life calculations.

The transition-to-locking regime depends very much on the fabric conditions and pre-tension (not accounted for in the calculations). This most probably explains the fact that in *TexMind* calculations, the force is the same in both directions: *TexMind* model operates with ideal distances between the filaments in the loop contacts. In the XCT-based model apparently the fabric is looser in X than in Y direction, which also corresponds to the behavior described by the manufacturer (dyna-mesh.com) The pre-tension will be “the must” for the experimental measurements and for the future modelling, as it allows stabilization of the initial tension conditions.

Summary

We have created geometrical and mechanical models for warp-knitted abdominal wall meshes. The models are built as “digital twins” with the help of 3D imaging with XCT, and using design of 3D mesh structures with *TexMind* software. XCT represents exact knitting pattern, so should theoretically result in the most accurate simulations. *TexMind* possesses the ability to virtually tweak the knitting pattern and, in that way, to optimize the pattern in terms of mechanical behavior. As such, we would able to optimize current mesh designs, or even come up with new mesh patterns that more closely resemble the mechanical behaviour of native fascia tissue.

We developed a methodology of 3D image acquisition of surgical abdominal meshes with XCT and methods and routines for creation of FE models for the real meshes on micro-level. The analysis of the mechanical behavior of a complex mesh under biaxial tension is feasible, whilst important difficulties are identified for development of true-to-life finite elements modelling. In future work, the limitations of the present study will be tackled to obtain models of the larger part of the mesh (as in Fig. 1b), a more precise reproduction of the knitting pattern and an experimental validation of the mechanical properties.

Acknowledgements

The FWO large infrastructure I013518N project is acknowledged for their financial support of the X-ray infrastructure and the KU Leuven XCT Core facility is acknowledged for the 3D image acquisition and quantitative post-processing tools (https://xct.kuleuven.be/).

References

[1] C. Towsend, Chapter 13: Surgery in the geriatric patient, in Sabiston Textbook of Surgery: The Biological Basis of Modern Surgical Practice, Elsevier, 2022.

[2] N.A. Henriksen, A. Montgomery, R. Kaufmann, F. Berrevoet, B. East, J. Fischer, W. Hope, D. Klassen, R. Lorenz, Y. Renard, M.A. Garcia Urena, M.P. Simons, Guidelines for treatment of umbilical and epigastric hernias from the European Hernia Society and Americas Hernia Society, British Journal of Surgery 107 (2020) 171-190. https://doi.org/10.1002/bjs.11489

[3] M.P.Simons, M. Smietanski, H.J. Bonjer, R. Bittner, M. Miserez, T.J. Aufenacker, R.J. Fitzgibbons, P.K. Chowbey, H.M. Tran, R. Sani, F. Berrevoet, J. Bingener, T. Bisgaard, K. Bury, G. Campanelli, D.C. Chen, J. Conze, D. Cuccurullo, A.C. de Beaux, H.H. Eker, R.H. Fortelny, J.F. Gillion, B.J. van den Heuvel, W.W. Hope, L.N. Jorgensen, U. Klinge, F. Köckerling, J.F. Kukleta, I. Konate, A.L. Liem, D. Lomanto, M.J.A. Loos, M. Lopez-Cano, M.C. Misra, A. Montgomery, S. Morales-Conde, F.E. Muysoms, H. Niebuhr, P. Nordin, M. Pawlak, G.H. van Ramshorst, W.M.J. Reinpold, D.L. Sanders, N. Schouten, S. Smedberg, R.K.J. Simmermacher, S. Tumtavitikul, N. van Veenendaal, D. Weyhe, A.R. Wijsmuller, The HerniaSurge Group, International guidelines for groin hernia management, Hernia 22 (2018) 1-165. https://doi.org/10.1007/s10029-017-1668-x

[4] D. Le, C.W. Deveney, N.L. Reaven, S.E. Funk, K.J. McGaughey, R.G. Martindale, Mesh choice in ventral hernia repair: so many choices, so little time, The American J. Surg. 205 (2013) 602-607. https://doi.org/10.1016/j.amjsurg.2013.01.026

[5] L. Miao, F. Wang, L. Wang, T. Zou, G. Brochu, R. Guidoin, Physical Characteristics of Medical Textile Prostheses Designed for Hernia Repair: A Comprehensive Analysis of Select Commercial Devices, Materials 8 (2015) 8148-8168 https://doi.org/10.3390/ma8125453

[6] N. Sanbhal, L. Miao, R. Xu, A. Khatri, L. Wang, Physical structure and mechanical properties of knitted hernia mesh materials: A review, J. Industr. Text. 48 (2017) 333-360. https://doi.org/10.1177/1528083717690613

[7] W.S. Cobb, J.M. Burns, K.W. Kercher, B.D. Matthews, H. James Norton, B. Todd Heniford, Normal Intraabdominal Pressure in Healthy Adults, J. Surgic. Res. 129 (2005) 231-235. https://doi.org/10.1016/j.jss.2005.06.015

[8] K. Baylón, P. Rodríguez-Camarillo, A. Elías-Zúñiga, J.A. Díaz-Elizondo, R. Gilkerson, K. Lozano, Past, present and future of surgical meshes: A review, Membranes 7 (2017) 47. https://doi.org/10.3390%2Fmembranes7030047

[9] X. Zhang, P. Ma, Application of knitting structure textiles in medical areas, Autex Res. J. 18 (2018) 181–191. https://doi.org/10.1515/aut-2017-0019

[10] Y. Kyosev, Warp Knitted Fabrics Construction, Milton: CRC Press LLC, 325, 2019

[11] L.-M. Zhu, P. Schuster, U. Klinge, Mesh implants: an overview of crucial mesh parameters, World journal of gastrointestinal surgery 7 (2015) 226. https://doi.org/10.4240%2Fwjgs.v7.i10.226

[12] B. Hernández-Gascón, E. Peña, G. Pascual, M. Rodríguez, J.M. Bellón, B. Calvo, Long-term anisotropic mechanical response of surgical meshes used to repair abdominal wall defects, J. Mech. Behav. Biomed. Mater. 5 (2012) 257-271. https://doi.org/10.1016/j.jmbbm.2011.09.005

[13] M.S. Yeoman, D. Reddy, H.C. Bowles, D. Bezuidenhout, P. Zilla, and T. Franz, A constitutive model for the warp-weft coupled non-linear behavior of knitted biomedical textiles, Biomaterials 31 (2010) 8484-8493. https://doi.org/10.1016/j.biomaterials.2010.07.033

[14] E. Pena, B. Hernandez-Gascon, and B. Calvo, Human abdomen: Mechanical modeling and clinical applications. Biomechanics of Living Organs: Hyperelastic Constitutive Laws for Finite Element Modeling, ed. Y. Payan and J. Ohayon, 2017, pp. 267-285.
[15] A. Tomaszewska, D. Reznikov, Combined numerical and experimental approach to determine numerical model of abdominal scaffold, Comput. Methods Biomech. Biomed. Engin. 25 (2022) 1235-1248. https://doi.org/10.1080/10255842.2021.2005788
[16] B. Hernandez-Gascon, N. Espes, E. Pena, G. Pascual, J.M. Bellon, B. Calvo, Computational framework to model and design surgical meshes for hernia repair, Comput. Methods Biomech. Biomed. Engin. 17 (2014) 1071-1085. https://doi.org/10.1080/10255842.2012.736967
[17] Y. Kyosev, Topology-Based Modeling of Textile Structures and Their Joint Assemblies: Principles, Algorithms and Limitations, Springer eBook Collection. Cham: Springer International Publishing, 238, 2019
[18] S. Sha, A. Geng, Y. Gao, B. Li, X. Jiang, H. Tao, L. Luo, X. Yuan, H. Ke et al., Review on the 3-D simulation for weft knitted fabric, J. Engin. Fibers Fabrics 16 (2021) 15589250211012528.
[19] H. Liu, Y. Kyosev, G. Jiang, Yarn level simulation of warp-knitted clothing elements – first results and challen ges, Communic. Develop. Assembl. Text. Products 3 (2022) 115-126. https://doi.org/10.25367/cdatp.2022.3.
[20] Y. Kyosev, TexMind Warp Knitting Editor 3D, TexMind UG: Heidenau, 2022.
[21] N. Naouar, D. Vasiukov, C.H. Park, S.V. Lomov, P. Boisse, Meso-FE modelling of textile composites and X-ray tomography, J. Mater. Sci. 55 (2020) 16969-16989. https://doi.org/10.1007/s10853-020-05225-x
[22] Harjkova, G., M. Barburski, S.V. Lomov, O. Kononova, and I. Verpoest, Weft knitted loop geometry measured with X-ray micro-computer tomography. Textile Research Journal, 2014. 84: pp. 500-512.
[23] P. Boisse, R. Akkerman, P. Carlone, L. Karger, S.V. Lomov, J. Sherwood, Advances in composite forming through 25 years of ESAFORM, Int. J. Mater. Forming 15 (2022) 39. http://doi.org/10.1007/s12289-022-01682-8
[24] DynaMesh. Tailored Implants Made of PVDF. 2022 [cited 2022 14/11/2022]; Information on: https://en.dyna-mesh.com/company-gb/.
[25] H. Wang, B. Klosterhalfen, A. Müllen, T. Otto, A. Dievernich, S. Jockenhövel, Degradation resistance of PVDF mesh in vivo in comparison to PP mesh, J. Mech. Behav. Biomed. Mater. 119 (2021) 104490. https://doi.org/10.1016/j.jmbbm.2021.104490
[26] C.D. Klink, K. Junge, M. Binnebösel, H.P. Alizai, J. Otto, U.P. Neumann, U. Klinge, Comparison of Long-Term Biocompability of PVDF and PP Meshes, J. Invest. Surgery 24 (2011) 292-299. https://doi.org/10.3109/08941939.2011.589883